Mathematical modeling of the effects of Wnt-10b on bone metabolism

Carley V. Cook[a,b], Mohammad Aminul Islam[a,b], Brenda J. Smith[c], Ashlee N. Ford Versypt[a,b,d,*]

[a] *School of Chemical Engineering, Oklahoma State University, Stillwater, OK, USA*
[b] *Department of Chemical and Biological Engineering, University at Buffalo, The State University of New York, Buffalo, NY, USA*
[c] *Department of Nutritional Sciences, Oklahoma State University, Stillwater, OK, USA*
[d] *Institute for Computational and Data Sciences, University at Buffalo, The State University of New York, Buffalo, NY, USA*

Abstract

Bone health is determined by many factors including bone metabolism or remodeling. Wnt-10b has been shown to alter osteoblastogenesis through pre-osteoblast proliferation and differentiation as well as the osteoblast apoptosis rate, which collectively lead to the increase of bone density. To model this change, we adapted a previously published model of bone remodeling. The resulting model is a single compartment system that includes ordinary differential equations for active osteoclasts, pre-osteoblasts, osteoblasts, and osteocytes and a differential equation that tracks the amount of bone present at the remodeling site. Our alterations to the original model consist of extending it past a single remodeling cycle and implementing a direct relationship to Wnt-10b. Four new parameters were estimated and validated using normalized data from mice. The model connects Wnt-10b to bone metabolism and predicts the change in bone volume caused by a change in Wnt-10b. We find that this model predicts the expected increase in pre-osteoblasts and osteoblasts while also pointing to a decrease in osteoclasts when Wnt-10b is increased.

Keywords: Bone remodeling, Wnt signaling, Mathematical modeling, Bone cells

1. Introduction

Osteoporosis is a disease characterized by decreased bone mass caused by the structural deterioration of bone tissue. The structure of healthy bone is a dense matrix with small pockets of space, but as osteoporosis breaks down the matrix, bone structure becomes less connected with larger pockets of space. Bone metabolism or remodeling is the process that replenishes existing bone tissue with new tissue. Homeostasis or no net change in volume or density of bone is achieved when the interactions are balanced between degradation and formation. When the balance is perturbed, bone tissue no longer remodels properly. The cells involved in remodeling are part of what is called a basic multicellular unit (BMU). For trabecular bone, the BMU works on the surface of the bone. The four main cells in a BMU are osteoclasts, pre-osteoblasts,

*Corresponding author: A. N. Ford Versypt ashleefv@buffalo.edu

osteoblasts, and osteocytes. Osteoclasts are responsible for breaking down the mineralized bone matrix in the resorption phase. Pre-osteoblasts differentiate into osteoblasts. Osteoblasts rebuild the bone matrix in the formation phase. Osteocytes are a form of osteoblasts that have been embedded in the bone matrix during the termination phase. While healthy they emit signals that help terminate the remodeling cycle and prevent a new remodeling cycle from occurring. When these cells become damaged or die, they release a signal that triggers a new remodeling cycle [1–4].

Wnt-10b is a signaling protein that interacts with cells involved in maintaining bone metabolism and is also important to the immune system. This protein can be produced by a number of different cells, including osteoblasts and T cells. A change in Wnt-10b levels has been shown to alter the bone volume significantly [5, 6]. Wnt-10b regulation of bone volume is attributed to a change of osteoblastogenesis and osteoblast apoptosis [7, 8]. The extent to which Wnt-10b alters these variables and how these alterations affect the cell populations and bone volume as a whole is currently unknown.

Currently, there are a few published mathematical/computational models on bone metabolism, One model describes the autocrine and paracrine interactions of osteoblasts and osteoclasts using ordinary differential equations (ODEs) that track the cell populations as well as changes in bone mass [9]. This model was later updated to include a relationship with the parathyroid hormone (PTH) [10]. These publications along with a model that tracks spatial bone volume changes [11] were used to develop a human based ODE model that tracks how different signals cause the development of active osteoclasts and osteoblasts and a change in trabecular bone mass [12]. None of these models include Wnt-10b in them; therefore, they lack a vital part of the bone remodeling system. The importance of including Wnt-10b in a bone remodeling model has been illustrated by a published network model that identified the Wnt and PTH pathways as the most important systems in regulating bone remodeling through a parameter sensitivity analysis [13].

A few of the existing bone metabolism models do explore the role Wnt-10b has in bone remodeling [14–18]. However, the models in one subset [15, 17, 18] assume a constant basal concentration of Wnt-10b and focus on how an increase of sclerostin competes for the Wnt binding sites. The models in the other subset [14, 16] allow the Wnt-10b concentration to vary but only in the presence of a tumor. These models connect Wnt-10b through Hill functions that alter an assortment of the terms for pre-osteoblast proliferation, differentiation from pre-osteoblasts to osteoblasts, and osteoblast apoptosis (Table 1).

The present work aims to improve understanding of bone metabolism by developing a model that directly connects the remodeling cycle to altered Wnt-10b concentrations that can be constant or dynamically induced by other physiologically processes. The model development is covered in Section 2, which includes an overview of the model, the data used for the model, and the techniques used to determine parameter values. After validating the model, we used it to explore how Wnt-10b directly effects important cell populations in a BMU and how these population changes alter bone volume (Section 3). The model will allow us to explore in the future potential ways to shift bone metabolism away from over resorption to

Table 1: Wnt-10b relationships presented in existing models for bone remodeling

Model	Wnt-10b type	Wnt-10b interactions
[14]	Dynamic	Pre-osteoblast proliferation
[15]	Constant	Not explicitly modeled
[16]	Dynamic	Pre-osteoblast proliferation
		Pre-osteoblast differentiation
[17]	Constant	Pre-osteoblast proliferation
[18]	Constant	Pre-osteoblast proliferation
		Pre-osteoblast differentiation
		Osteoblast apoptosis

prevent or repair bone damage caused by osteoporosis but not without some limitations discussed in Section 4.

2. Methods

We altered a published model, which is referred to as Graham 2013 [12], to include a mathematical relationship that represents how Wnt-10b interacts with bone formation. This is a single compartment model that tracks the important cells involved in the bone remodeling cycle as well as bone volume. We extended past a single remodeling cycle and added a direct relationship to Wnt-10b stimuli. We added a relationship to Wnt-10b by utilizing published data to obtain parameters that were fitted utilizing MATLAB nonlinear least-squares solver `lsqcurvefit` and ODE solver `ode15s` with the `NonNegative` option turned on. This option ensures that the model does not attempt to push the populations or bone volume below zero as this is not physiological.

2.1. Graham 2013 model

The Graham 2013 model we utilized includes five ODEs that track the changes in bone volume (z) through the active populations of osteocytes (S), pre-osteoblasts (P), osteoblasts (B), and osteoclasts (C) [12]. The model does not include an equation for the population of pre-osteoclasts. The model includes important autocrine and paracrine signaling factors that are represented by power law relationships (Figure 1), g_{ij} and f_{ij}, where i and j are the two cell types involved in the signaling. This section summarizes the parts of the Graham 2013 model and parameter values that we adopted directly from [12] without alteration (Table 2).

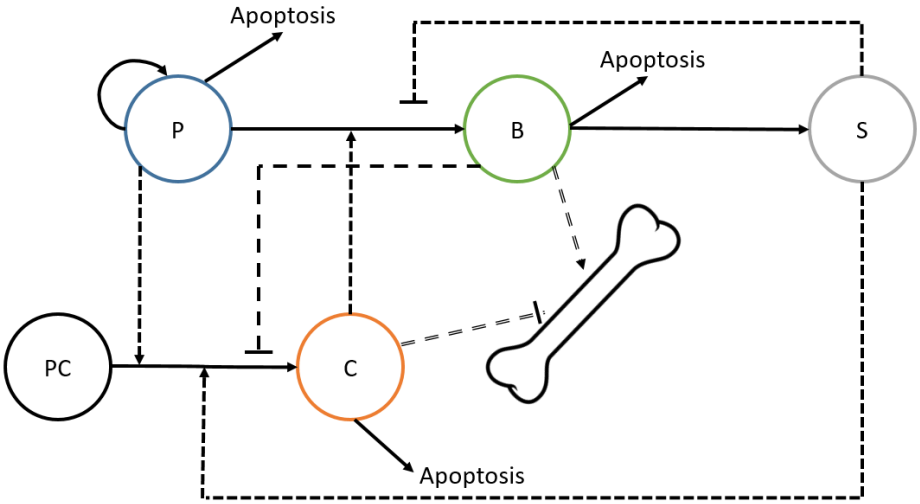

Figure 1: Interactions between bone cell populations considered in the Graham 2013 model [12]. Pre-osteoblasts (P), osteoblasts (B), osteocytes (S), and osteoclasts (C) are tracked by differential equations. Pre-osteoclasts (PC) are assumed constant and are not explicitly modeled. The interactions include an assortment of autocrine (not depicted here) and paracrine (single dashed lines) signaling factors. The single dashed lines with arrows represent an activating relationship, and the single dashed lines with a block end represent an inhibitory relationship. The solid lines with arrows represent the transformation or proliferation of a cell type. Impacts of bone cells on bone volume from a combination of bone resorption and formation are represented by double dashed lines with block and arrow ends, respectively.

2.1.1. Osteocytes

Equation 1 describes the dynamics of the osteocyte cell population, S. Mature osteoblasts convert into osteocytes at a rate of α_1. The term $\left(1 - \frac{S}{K_s}\right)_+$ represents the effectiveness of sclerostin regulation by osteocytes, and the subscript $+$ means that the value must remain greater than or equal to zero. If the quantity inside the parentheses were to be evaluated as ¡0, then the term would be set to 0. Note that although sclerostin regulation does include a Wnt pathway, we are focusing on Wnt-10b excreted from T cells or from a genetic perturbation, not Wnt-10b produced within a normal balanced remodeling cycle. It is assumed in the model that over the duration of remodeling, osteocytes will not die; therefore, there is no death term in the equation. Instead of a death term, the osteocyte population is reduced from the steady state value of 200 cells to 180 cells at the start of each remodeling cycle. This decrease in osteocyte population represents the initial biomechanical action that triggers a remodeling cycle.

$$\frac{dS}{dt} = \alpha_1 B^{g_{31}} \left(1 - \frac{S}{K_s}\right)_+ \tag{1}$$

2.1.2. Osteoclasts

Equation 2 describes the dynamics of the activated osteoclast cell population, C. A large amount of pre-osteoclasts are assumed to be available without a significant change in the population, so the pre-osteoclast

Table 2: Parameter values and definitions directly from [12]

Parameter	Definition	Value	Units
α_1	Osteoblast embedding rate	0.5	day^{-1}
α_2	Differentiation rate of pre-osteoblast precursors	0.1	day^{-1}
α_3	Pre-osteoblast proliferation rate	0.1	day^{-1}
α_4	Differentiation rate of osteoclast precursors	0.1	day^{-1}
β_1	Differentiation rate of pre-osteoblasts	0.1	day^{-1}
β_2	Osteoblast apoptosis rate	0.1	day^{-1}
δ	Pre-osteoblast apoptosis rate	0.1	day^{-1}
ϵ	Avoid 0 denominator	1	cells
K_s	Critical value of osteocyte population	200	cells
g_{31}	Osteoblast autocrine signaling	1	dimensionless
g_{21}	Osteocyte paracrine signaling of pre-osteoblasts	2	dimensionless
g_{22}	Sclerostin regulation of osteoblastogenesis	1	dimensionless
g_{32}	Pre-osteoblast autocrine signaling	1	dimensionless
g_{41}	Osteocyte paracrine signaling of osteoclasts	1	dimensionless
g_{42}	Pre-osteoblast paracrine signaling of osteoclasts	1	dimensionless
g_{43}	Osteoblast paracrine signaling of osteoclasts	-1	dimensionless
g_{44}	Sclerostin regulation of osteoclastogenesis	1	dimensionless
f_{12}	Pre-osteoblast paracrine signaling of osteoblasts	1	dimensionless
f_{14}	Osteoclast paracrine signaling of osteoblasts	1	dimensionless
f_{23}	Osteoblast autocrine signaling for apoptosis	1	dimensionless
f_{34}	Osteoclast autocrine signaling for apoptosis	1	dimensionless
k_1	Bone resorption rate	0.698331	$\%\text{volume}/\text{day}^2$
k_2	Balanced bone formation rate	0.015445	$\%\text{volume}/\text{day}^2$

Note: k_1 was manually adjusted from the rounded value of 0.7 reported in [12] to six significant figures as for k_2 to maintain no steady state change in bone volume at the end of a remodeling cycle (in the absence of Wnt-10b perturbations) when the populations of all cell types return to their initial conditions.

population is not modeled. The production of osteoclasts depends on a differentiation rate of α_4 and an interaction of the receptor activator of NF-κB (RANK)/RANK ligand (RANKL)/osteoprotegerin (OPG) system that is described by the term $S^{g_{41}}P^{g_{42}}(\epsilon+B)^{g_{43}}\left(1-\frac{S}{K_s}\right)_+^{g_{44}}$. OPG from osteoblasts can act as a decoy receptor for RANKL. This interaction is represented as $(\epsilon+B)^{g_{43}}$. This term includes a very small number, ϵ, to prevent dividing by zero when the osteoblast population is zero, since g_{43} is a negative integer. The second part of the equation represents osteoclast apoptosis with a first order rate constant β_3.

$$\frac{dC}{dt} = \alpha_4 S^{g_{41}}P^{g_{42}}(\epsilon+B)^{g_{43}}\left(1-\frac{S}{K_s}\right)_+^{g_{44}} - \beta_3 C^{f_{34}} \tag{2}$$

2.2. Model enhancements for Wnt-10b dependence

This section covers the parts of the model that we altered to explicitly account for Wnt-10b changes from stimuli outside the normal bone remodeling cycle. Many parts of the equations remain the same as the Graham 2013 model (Table 2), but with new terms added to or parameters adjusted in each of the following equations (Table 4). The adjusted parameters are denoted with the subscript *adj*. As these additions are related to Wnt-10b, we introduce a variable, Wnt, into the equations that represents the normalized fold change of Wnt-10b present compared to the normal levels of Wnt-10b in the system. Note that if the Wnt-10b levels are normal, the remodeling cycle is normal as well, and Wnt takes on a value of zero. Figure 2 visually describes how Wnt-10b alters the remodeling cycle.

We connected the concentration of Wnt-10b to the remodeling cycle through a Hill function in the form of

$$\pi_{Wnt} = \frac{Wnt}{K_M + Wnt} \tag{3}$$

We assume that K_M remains the same for both the pre-osteoblast and osteoblast interactions because they are both from osteoblast lineage. A Hill function relationship was chosen based on the previous models related to Wnt-10b (Table 1). This particular form was chosen so that when the Wnt-10b concentration is not perturbed, π_{Wnt} will take the value of zero, and the model will return to a steady state of no net bone volume change at the end of a remodeling cycle.

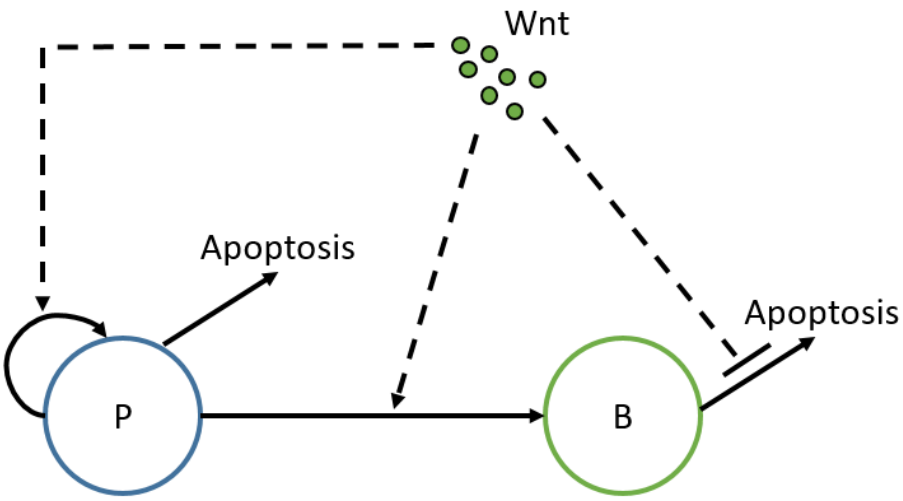

Figure 2: Wnt-10b impacts on bone metabolism. Wnt-10b (Wnt) stimulates osteoblastogenesis through pre-osteoblast (P) proliferation and differentiation to osteoblasts. Wnt-10b inhibits osteoblast (B) apoptosis. The solid lines with arrows represent the transformation or proliferation of a cell type. The Wnt-10b signaling relationships are shown by dashed lines, where arrows represent activation and blocks ends represent inhibition.

Table 3: Initial conditions for ordinary differential equations

Symbol	Initial condition	Definition	Units
S	180	Osteocyte population at time t	cells
P	0	Pre-osteoblast population at time t	cells
B	0	Osteoblast population at time t	cells
C	0	Osteoclast population at time t	cells
z	100	Relative bone volume at time t	%

Table 4: Estimated parameter values and definitions

Parameter	Definition	Value	Units
α_{3adj}	Wnt-10b dependent pre-osteoblast proliferation rate	6.47×10^{-1}	day^{-1}
β_{1adj}	Wnt-10b dependent differentiation rate of pre-osteoblasts	4.96×10^{-1}	day^{-1}
β_{2adj}	Wnt-10b dependent osteoblast apoptosis rate	2.30×10^{-3}	day^{-1}
K_M	Half saturation for Wnt-10b	27.6	dimensionless

2.2.1. Pre-osteoblasts

Equation 4 describes the dynamics of the pre-osteoblast cell population, P. The first four terms are unchanged from the Graham 2013 model. Pre-osteoblasts differentiate at a rate of α_2 from a large population of stem cells. This differentiation is triggered by the sclerostin signaling of osteocytes. The pre-osteoblast cell population can also be increased by proliferation of existing cells at a rate of α_3. The pre-osteoblast population is decreased by differentiation into osteoblasts regulated by paracrine signals from the osteoclast population and by apoptosis with a first order rate constant of δ. We have altered the equation from Graham 2013 to include a Hill function relationship with Wnt-10b in the pre-osteoblast proliferation and pre-osteoblast differentiation to osteoblasts processes. The fifth term in Equation 4 represents the increase in pre-osteoblast proliferation rate due to excess Wnt-10b. The sixth term quantifies Wnt-10b direct effects on pre-osteoblast differentiation independent from osteoclast regulation.

$$\frac{dP}{dt} = \alpha_2 S^{g_{21}} \left(1 - \frac{S}{K_s}\right)_+^{g_{22}} + \alpha_3 P^{g_{32}} \left(1 - \frac{S}{K_s}\right)_+ - \beta_1 P^{f_{12}} C^{f_{14}} - \delta P + \alpha_{3adj} \pi_{Wnt} P - \beta_{1adj} \pi_{Wnt} P \quad (4)$$

2.2.2. Osteoblasts

Equation 5 describes the dynamics of the osteoblast cell population, B. Pre-osteoblasts mature into osteoblasts at a rate of β_1 with osteoclast regulation and normal Wnt-10b ($Wnt = 0$), but when the amount of Wnt-10b is altered, the maturation rate changes by $\beta_{1adj} Wnt$ as discussed above for Equation 4. Wnt-10b also changes how fast osteoblasts die. We reduced the osteoblast apoptosis rate constant β_2 by $\beta_{2adj} \pi_{Wnt}$. The final term in Equation 5 represents the conversion of osteoblasts into osteocytes.

$$\frac{dB}{dt} = \beta_1 P^{f_{12}} C^{f_{14}} + \beta_{1adj} \pi_{Wnt} P - (\beta_2 - \beta_{2adj} \pi_{Wnt}) B^{f_{23}} - \alpha_1 B^{g_{31}} \left(1 - \frac{S}{K_s}\right)_+ \quad (5)$$

2.2.3. Bone volume

Equation 6 shows the dynamics of bone volume at a single remodeling site. Bone volume is reduced by osteoclasts at a rate of k_1. This rate is slightly different than the rate in Graham 2013 due to rounding. In the Graham model, the reported k_1 value resulted in a slightly unbalanced remodeling cycle (a new steady state resulted at the end of each cycle and amplified after repeated cycles). We manually adjusted k_1 to match the same number of significant figures as k_2 until we obtained a completely balanced remodeling cycle–that is, no steady state change in bone volume at the end of one remodeling cycle (in the absence of Wnt-10b perturbations) when the populations of all cell types return to their initial conditions. Note that this alteration is not related to a change in Wnt-10b concentrations. Osteoblasts build back the bone at a rate of k_2.

$$\frac{dz}{dt} = -k_1 C + k_2 B \quad (6)$$

2.3. Mouse data

This section covers the data used and the assumptions made concerning the data during the development of the model. If the data was originally presented in a graph, then it was extracted using Plot Digitizer (version 2.6.8) [19], a tool that digitizes the axes and returns the data points based on the pixel locations. We utilized three published data sources from *in vivo* experiments with C57BL/6 mice (Table 5). Two sources from the same lab [20, 21] were used to estimate the parameters, and the third source from another lab [22] was used to validate the model.

2.3.1. Bone volume

The $\frac{\text{bone volume}}{\text{total volume}}$ (BV/TV) data was normalized against the control groups using

$$\frac{\text{altered} - \text{baseline}}{\text{baseline}} * 100 = \text{normalized BV/TV} \tag{7}$$

turning BV/TV data into relative change in bone volume. We refer to "altered BV/TV" to denote mice that have been genetically altered to over- or under-produce Wnt-10b, while "baseline BV/TV" denotes unaltered litter mates. We normalized the mouse data for use in the model previously parameterized for humans. We make the assumption that the normalized BV/TV data is consistent from mice to human. Note that since our model starts at a baseline of 100 percent of normal bone volume, we expect our simulation to produce z that is 100 plus the expected normalized bone volume. We also took into account the different remodeling cycle lengths of our model and mice. Mice have a 12 to 15 day remodeling cycle, but our model has a one 100-day remodeling cycle for humans [23]. We held constant the number of remodeling cycles between mice and our model when comparing them. We assumed that the six and three month old mice could be modeled as having undergone six cycles. Thus we ran the computational model for six 100-day cycles.

2.3.2. Wnt-10b fold change

For our model, we took fold change of Wnt-10b to be

$$\frac{\text{altered levels} - \text{baseline levels}}{\text{baseline levels}} = \text{Normalized Wnt10b fold change} \tag{8}$$

Note that the notation for "altered" and "baseline" remains consistent with the previous section except Wnt-10b is in place of BV/TV. This was done so that the model would produce a balanced remodeling cycle (returning to initial steady state) when $Wnt = 0$, representing a normal baseline level of Wnt-10b.

2.4. Numerical methods

The system of ODEs for the populations of the bone cells and the bone volume in Equations 1–2 and 4–6 are solved simultaneously using the `ode15s` function in MATLAB, which is a variable-step, variable-order

Table 5: Bone volume data from mice with genetically altered Wnt-10b expression

Normalized Wnt-10b fold change	Age (months)	Altered BV/TV (%)	Baseline BV/TV (%)	Normalized BV/TV	Source
-1	3	4.3	7.4	-29.7	[21]
+1.8	3	8.04	6.35	26.6	[22]
+1.8	6	4.42	3.24	36.6	[22]
+5	3	18.1	10.7	69.2	[21]
+50	6	15.8	3.6	339	[20]

Note: To produce the 50-fold change of Wnt-10b in mice, [20] followed the procedures in [24].

solver based on numerical differentiation formulas of orders 1 to 5 for stiff problems. The relative tolerance is set to 10^{-7}. The time step is set adaptively by `ode15s`. The NonNegative option is turned on, because all of the dependent variables (cell populations and bone volume) must have strictly non-negative values physiologically.

2.5. Parameter estimation

We fit the parameters $\alpha_{3adj}, \beta_{1adj}, \beta_{2adj}$, and K_M using the MATLAB function `lsqcurvefit`. The multicycle effect of Wnt-10b should be on bone volume. Thus, we solve the system of ODEs using the numerical methods described in the previous section for multiple cycles. The ODE solver is called for one remodeling cycle at at a time. The solutions from the final time at the end of one cycle are used as the initial conditions for the subsequent cycle, except cell populations that have a value less than one are set to 0 to not allow fractional values less than 1 discrete cell to persist. The process is repeated for the integer number of cycles. The bone volume calculated at the end of the series of remodeling cycles is taken as the model output for the parameter estimation algorithm and is compared to the normalized BV/TV data. The input is the magnitude of normalized Wnt-10b fold change. We assumed that the saturation parameter K_M could take on a value between 1 and 100, and bounded the parameter fitting accordingly. We bounded β_{1adj} and $alpha_{3adj}$ between 0 and 1 based on the magnitudes of the other parameters. We checked that $beta_{1adj}$ is less than $alpha_{3adj}$ to ensure the total effect of increasing Wnt-10b on pre-osteoblasts yields a net increase in formation. Since β_{2adj} and β_2 collectively impact osteoblast apoptosis, we checked that the net apoptosis rate satisfies

$$\beta_2 - \beta_{2adj}\pi_{Wnt} \geq 0. \tag{9}$$

For `lsqcurvefit` the optimization options were set to have step tolerance of 10^{-16}, function tolerance of 10^{-14}, optimality tolerance of 10^{-6}, and 1000 maximum function evaluations.

3. Results and Discussion

Parameter estimation resulted in parameters (Table 4) that fit the data with a residual norm of 167.58 and visually agreed with the data from [20, 21] well (Figure 3).

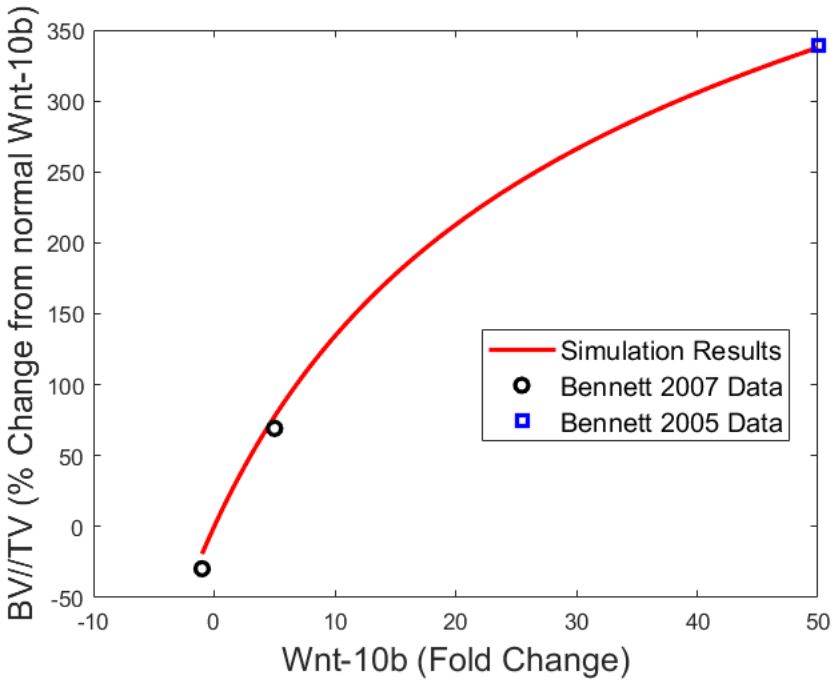

Figure 3: Normalized BV/TV relationship with normalized Wnt-10b fold change. The simulated results produce an acceptable residual norm of 167.58 with the data from [20, 21]. Data points were compared with the final simulated BV/TV after six remodeling cycles.

To determine if the model is a good predictor of the change in bone volume that occurs when Wnt-10b levels are perturbed, we utilized a separate set of data [22]. The simulation results fall within the error of the data at six and twelve remodeling cycles (Figure 4). This model validation is particularly good for 6 or fewer remodeling cycles.

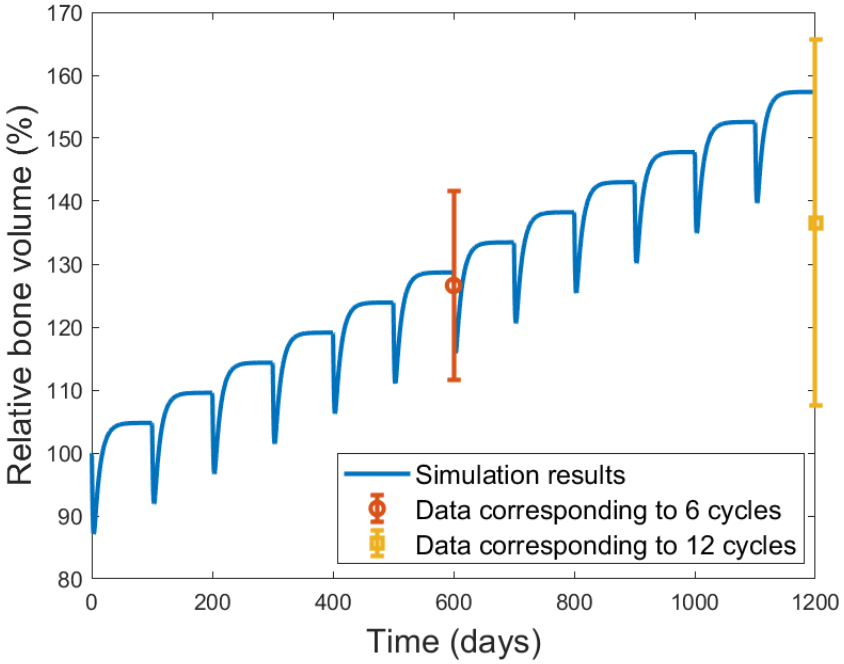

Figure 4: Validation of model with data from [22]. The simulation shown is the result of running the model with a 1.8 normalized fold change of Wnt-10b for twelve remodeling cycles. The data provided in [22] corresponds to six and twelve remodeling cycles. The simulation falls within the error of the data.

The model gives the results shown in Figure 5 for the bone volume progression over multiple remodeling cycles for the full range of Wnt-10b perturbations explored. The initial conditions for these simulations are provided in Table 3. As Wnt-10b increases, the bone volume also increases. For each fold change in Wnt-10b shown, we also determine the corresponding numbers of the activated populations of osteocytes, pre-osteoblasts, osteoblasts, and osteoclasts (Figure 6). The results show a positive correlation with pre-osteoblast and osteoblast populations and a slight negative correlation with osteoclasts (Figure 7). Even though we did not alter the osteoclast equation, the population is related to the ratio of pre-osteoblasts to osteoblasts. The model predicts that the ratio of pre-osteoblasts to osteoblasts and the ratio of osteoclasts to osteoblasts both decrease with increasing Wnt-10b (Figure 8). The cumulative numbers of cells of each type were determined by integrating the areas under the curves shown in Figure 7 using the `trapz` function in MATLAB. The areas under the curves were used for comparison instead of the dynamic number of cells given that the initial conditions for numbers of activated cells of all three types are 0.

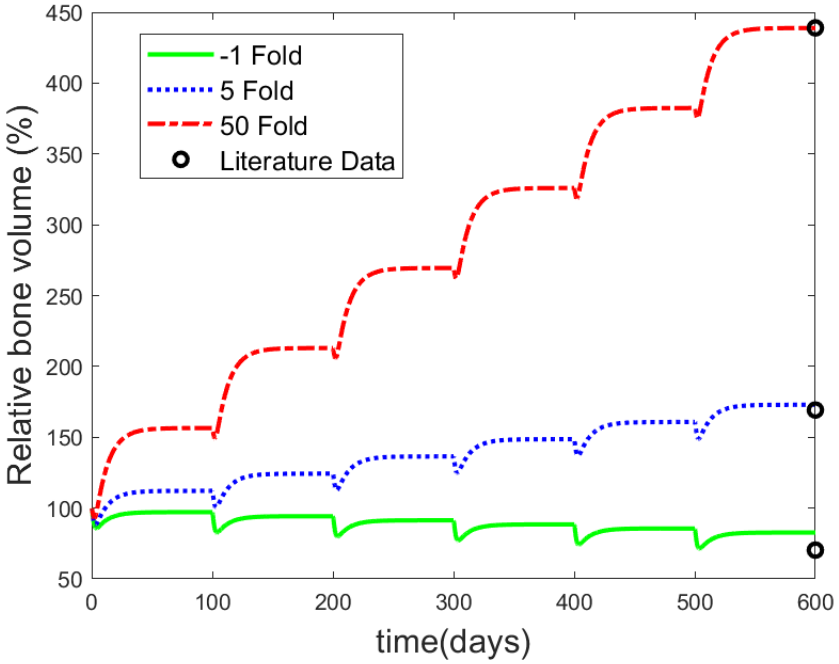

Figure 5: Simulation results for three normalized Wnt-10b fold changes shown in the legend. These specific fold changes were used to parameterize the model by comparison of the final bone volume with the corresponding data points from [20] and [21]. All three simulations were run for six remodeling cycles.

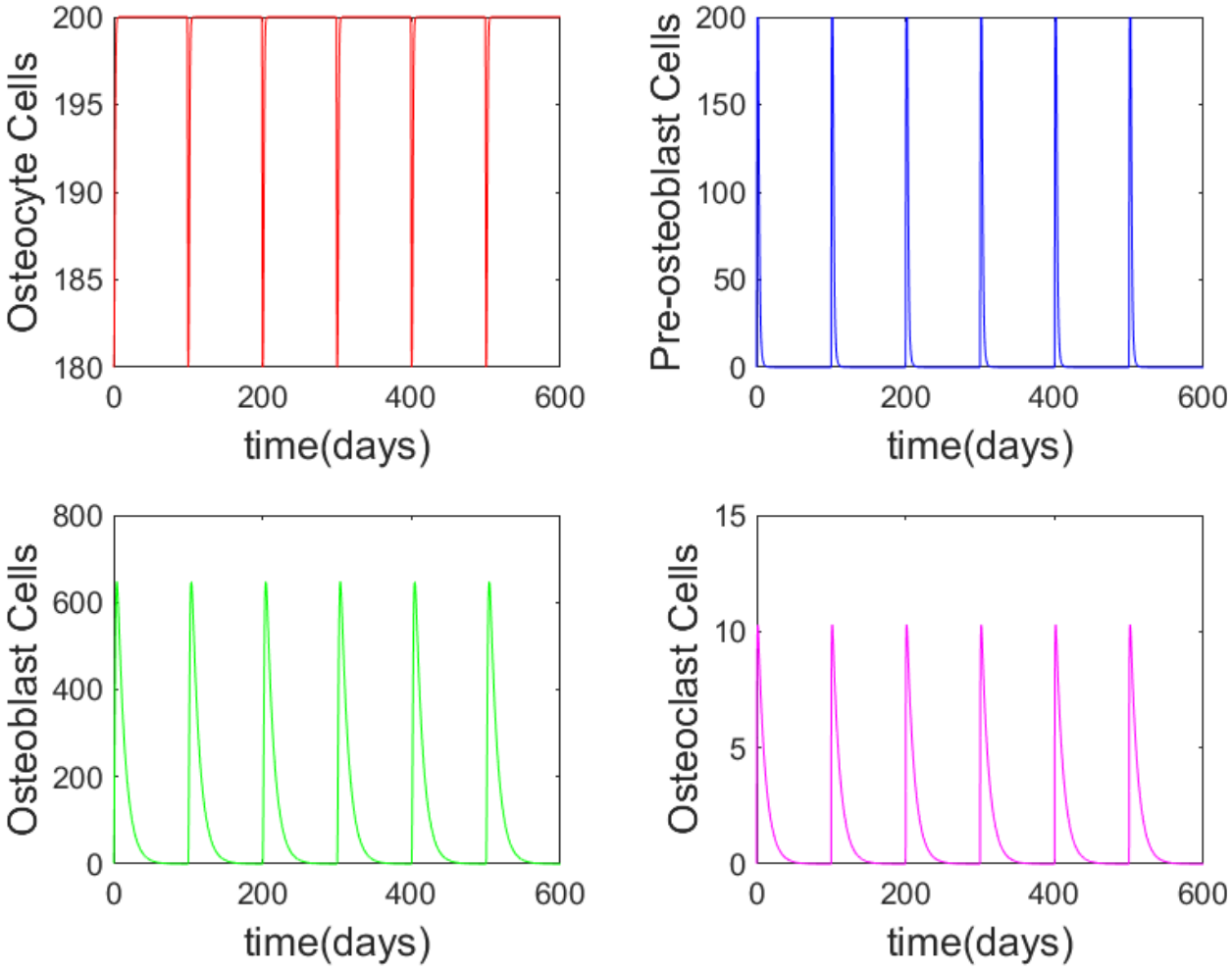

Figure 6: Activated cell population dynamic results for a normalized 50 fold increase in Wnt-10b. The activated cell populations follow identical dynamics for each remodeling cycle.

The reduction of osteoclasts population has been experimentally tested for mice with a normalized 5-fold increase in Wnt-10b; they found that the change in the number of osteoclasts on the perimeter of the bone was not statistically significant [21]. However, based on the physiology of bone remodeling, it is expected that a change in the ratio of pre-osteoblast and osteoblasts would alter osteoclast populations through the RANK/RANKL/OPG pathway [17, 25, 26]. In this pathway, pre-osteoblasts, osteoblasts, and osteocytes secrete RANKL that binds to RANK receptors on osteoclasts thus increasing osteoclastogenesis. Osteoblasts also secrete OPG, which is a competitive inhibitor of RANKL (Figure 9). It is also important to note that the predicted change in osteoclast population is still small enough that it would be hard to quantify experimentally. Determining the indirect relationship between activated osteoclast population and Wnt-10b would help to further validate the osteoclast population aspect of the model.

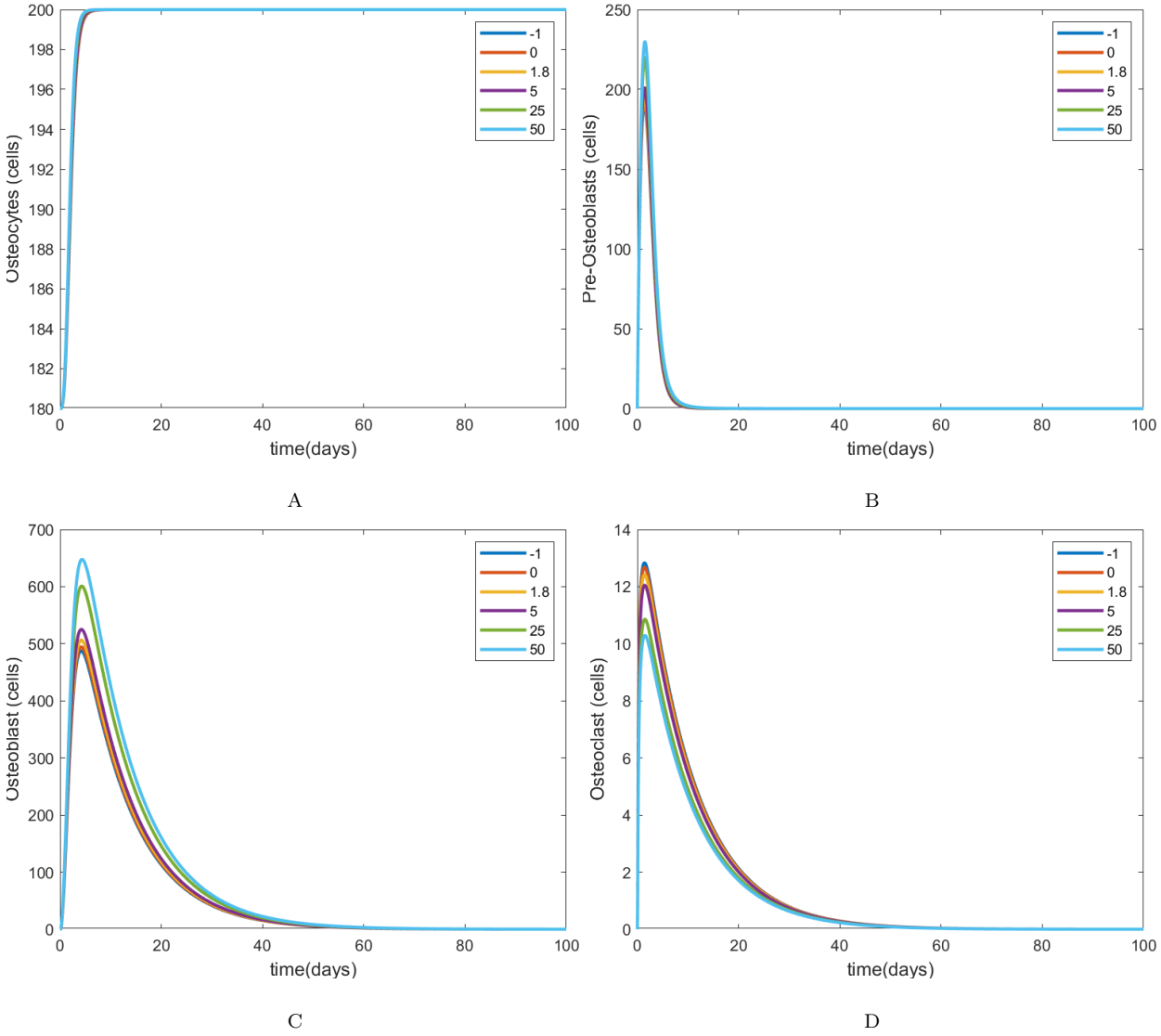

Figure 7: Activated cell population results for a single remodeling cycle with varying Wnt-10b concentrations shown in the legends. The osteocyte dynamics (A) show little change across Wnt-10b concentrations. The pre-osteoblast dynamics (B) and osteoblast dynamics (C) show a positive correlation with Wnt-10b. Osteoclasts (D) decrease with increasing Wnt-10b.

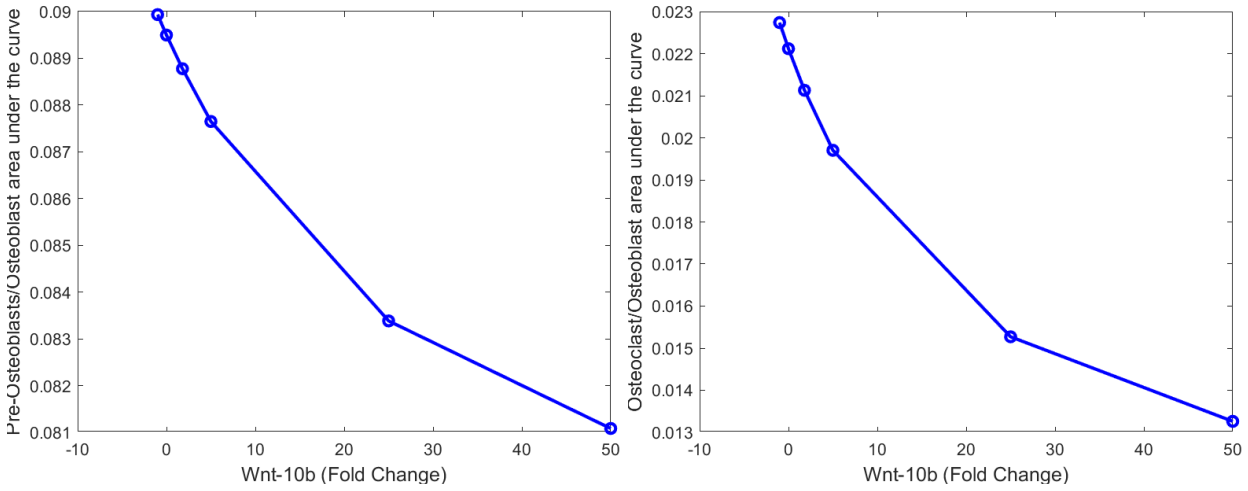

A B

Figure 8: Ratios of the cumulative numbers (area under the curve) of pre-osteoblasts (A) and osteoclasts (B) to osteoblasts. As Wnt-10b increases, both of the ratios decrease.

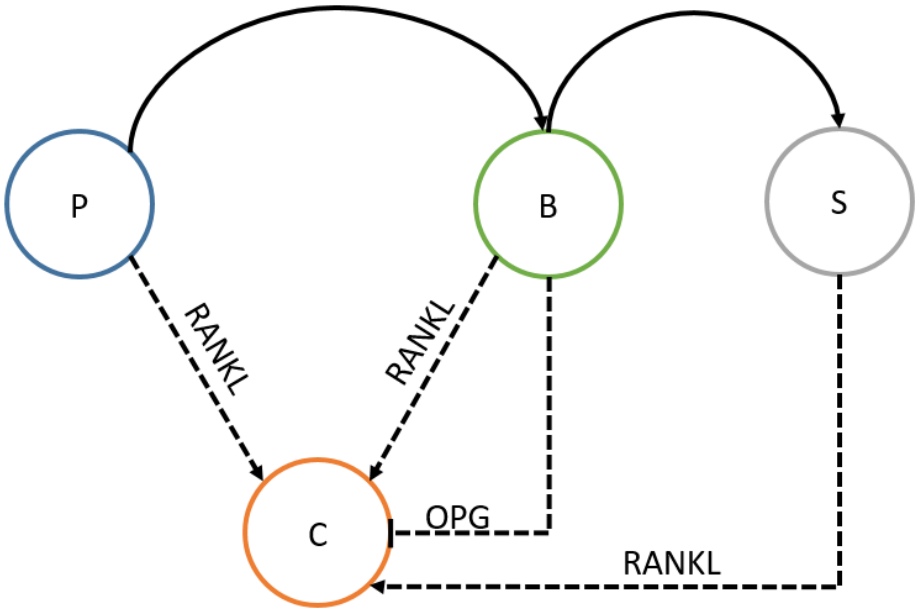

Figure 9: RANK/RANKL/OPG pathway where osteoblastic cell populations regulate the osteoclasts (C) cell populations. Pre-osteoblasts (P), osteoblasts (B), and osteocytes(S) secrete RANKL causing an increase in osteoclasts. Osteoblasts also inhibit osteoclastogenesis by secreting OPG, a competitive inhibitor of RANKL.

This model does provide insight into bone metabolism, but it is not without its limitations. The data utilized was normalized mice data, and the remodeling cycle was set to 100 days instead of a typical 200 day human remodeling time. These issues can be resolved if more data becomes available. In the future we would like to expand this model to include other direct relationships with biological chemicals of interest

such as TNF-α (experimentally shown to alter osteoclast formation and activity) and IL-6 (experimentally shown to alter osteoclast formation) [27].

4. Conclusion

Understanding the relationship between bone metabolism and Wnt-10b could lead to new ways to treat and prevent osteoporosis. Though there are a few published models about bone metabolism, the model developed here provides new insight on how chronic changes in Wnt-10b alter a single bone remodeling cycle or a sequence of cycles. Experimentally Wnt-10b has been shown to alter osteoblastogenesis and osteoblast apoptosis rates. Our model is able to reproduce the expected changes in pre-osteoblasts and osteoblasts and is able to predict changes in bone volume caused by Wnt-10b. Our model also points to a slight decrease in osteoclasts that is hard to determine experimentally but is mechanistically sound. These results could be used to design future experiments that could further enhance understanding of the Wnt-10b and bone metabolism relationship.

References

[1] A. Parfitt, Targeted and nontargeted bone remodeling: relationship to basic multicellular unit origination and progression, Bone 30 (1) (2002) 5–7.

[2] A. M. Parfitt, Osteonal and hemi-osteonal remodeling: the spatial and temporal framework for signal traffic in adult human bone, J. Cell. Biochem. 55 (3) (1994) 273–286.

[3] E. F. Eriksen, Cellular mechanisms of bone remodeling, Rev. Endocr. Metab. Disord. 11 (4) (2010) 219–227.

[4] L. J. Raggatt, N. C. Partridge, Cellular and molecular mechanisms of bone remodeling, J. Biol. Chem. 285 (33) (2010) 25103–25108.

[5] M. Kato, M. S. Patel, R. Levasseur, I. Lobov, B. H.-J. Chang, D. A. Glass, C. Hartmann, L. Li, T.-H. Hwang, C. F. Brayton, et al., Cbfa1-independent decrease in osteoblast proliferation, osteopenia, and persistent embryonic eye vascularization in mice deficient in Lrp5, a Wnt coreceptor, J. Cell Biol. 157 (2) (2002) 303–314.

[6] J. M. Patsch, T. Kohler, A. Berzlanovich, C. Muschitz, C. Bieglmayr, P. Roschger, H. Resch, P. Pietschmann, Trabecular bone microstructure and local gene expression in iliac crest biopsies of men with idiopathic osteoporosis, J. Bone Miner. Res. 26 (7) (2011) 1584–1592.

[7] P. Wend, K. Wend, S. Krum, G. Miranda-Carboni, The role of Wnt-10b in physiology and disease, Acta Physiol. 204 (1) (2012) 34–51.

[8] H. Jing, X. Su, B. Gao, Y. Shuai, J. Chen, Z. Deng, L. Liao, Y. Jin, Epigenetic inhibition of Wnt pathway suppresses osteogenic differentiation of BMSCs during osteoporosis, Cell Death Dis. 9 (2) (2018) 1–12.

[9] S. V. Komarova, R. J. Smith, S. J. Dixon, S. M. Sims, L. M. Wahl, Mathematical model predicts a critical role for osteoclast autocrine regulation in the control of bone remodeling, Bone 33 (2) (2003) 206–215.

[10] S. V. Komarova, Mathematical model of paracrine interactions between osteoclasts and osteoblasts predicts anabolic action of parathyroid hormone on bone, Endocrinology 146 (8) (2005) 3589–3595.

[11] B. P. Ayati, C. M. Edwards, G. F. Webb, J. P. Wikswo, A mathematical model of bone remodeling dynamics for normal bone cell populations and myeloma bone disease, Biol. Direct 5 (1) (2010) 28.

[12] J. Graham, B. Ayati, S. Holstein, J. Martin, The role of osteocytes in targeted bone remodeling: a mathematical model, PLoS ONE 8 (5).

[13] C. J. Proctor, A. Gartland, Simulated interventions to ameliorate age-related bone loss indicate the importance of timing. front endocrinol (lausanne). 2016; 7: 61, Front. Endocrinol. 7 (2016) 61.

[14] P. R. Buenzli, P. Pivonka, B. S. Gardiner, D. W. Smith, Modelling the anabolic response of bone using a cell population model, J. Theor. Biol. 307 (2012) 42–52.

[15] R. J. Eudy, M. R. Gastonguay, K. T. Baron, M. M. Riggs, Connecting the dots: Linking osteocyte activity and therapeutic modulation of sclerostin by extending a multiscale systems model, CPT: Pharmacometrics Syst. Pharmacol. 4 (9) (2015) 527–536.

[16] A. Farhat, D. Jiang, D. Cui, E. T. Keller, T. L. Jackson, An integrative model of prostate cancer interaction with the bone microenvironment, Math. Biosci. 294 (2017) 1–14.

[17] M. Martin, V. Sansalone, D. M. L. Cooper, M. R. Forwood, P. Pivonka, Mechanobiological osteocyte feedback drives mechanostat regulation of bone in a multiscale computational model, Biomech. Model. Mechanobiol. 18 (5) (2019) 1475–1496.

[18] V. Lemaire, D. R. Cox, Dynamics of bone cell interactions and differential responses to PTH and antibody-based therapies, Bull. Math. Biol. 81 (9) (2019) 3575–3622.

[19] Huwaldt, J. A., Plot Digitizer, `https://sourceforge.net/projects/plotdigitizer/files/plotdigitizer/2.6.8/` (2015 (accessed June 12, 2021)).

[20] C. N. Bennett, K. A. Longo, W. S. Wright, L. J. Suva, T. F. Lane, K. D. Hankenson, O. A. MacDougald, Regulation of osteoblastogenesis and bone mass by Wnt-10b, Proc. Natl. Acad. Sci. U. S. A. 102 (9) (2005) 3324–3329.

[21] C. N. Bennett, H. Ouyang, Y. L. Ma, Q. Zeng, I. Gerin, K. M. Sousa, T. F. Lane, V. Krishnan, K. D. Hankenson, O. A. MacDougald, Wnt-10b increases postnatal bone formation by enhancing osteoblast differentiation, J. Bone Miner. Res. 22 (12) (2007) 1924–1932.

[22] S. Roser-Page, T. Vikulina, M. Zayzafoon, M. N. Weitzmann, CTLA-4Ig-induced T cell anergy promotes Wnt-10b production and bone formation in a mouse model, Arthritis Rheumatol. 66 (4) (2014) 990–999.

[23] R. L. Jilka, The relevance of mouse models for investigating age-related bone loss in humans, J. Gerontol. A Biol. Sci. Med. Sci. 68 (10) (2013) 1209–1217.

[24] K. A. Longo, W. S. Wright, S. Kang, I. Gerin, S.-H. Chiang, P. C. Lucas, M. R. Opp, O. A. MacDougald, Wnt-10b inhibits development of white and brown adipose tissues, J. Biol. Chem. 279 (34) (2004) 35503–35509.

[25] J. M. Kim, C. J. Lin, Z. Stavre, M. B. Greenblatt, J. H. Shim, Osteoblast-osteoclast communication and bone homeostasis, Cells 9 (9).

[26] T. J. Martin, G. A. Rodan, Intercellular Communication during Bone Remodeling, Elsevier, 2008, pp. 547–560.

[27] M. Ponzetti, N. Rucci, Updates on osteoimmunology: what's new on the cross-talk between bone and immune system, Front. Endocrinol. 10 (2019) 236.